J Mater Sci: Mater Electron (2016) 27:11110–11117
DOI 10.1007/s10854-016-5228-4

Effect of $NdAlO_3$ on microstructure, dielectric properties and temperature-stable mechanism of (Sr, Ca, Nd)TiO_3 ceramics at microwave frequency

Jingjing Qu[1] · Delong Huang[1] · Xing Wei[1] · Fei Liu[2,3] · Changlai Yuan[2] · Bailin Qin[2]

Received: 5 April 2016 / Accepted: 20 June 2016 / Published online: 23 June 2016

Abstract Microwave dielectric ceramics $(1-x)(Sr_{0.3}Ca_{0.427}Nd_{0.182})TiO_3$–$xNdAlO_3$ (abbreviated as SCNTAx hereafter, $0.1 \leq x \leq 0.4$) were prepared by conventional mixed oxide route, and their phase composition, microstructure and microwave dielectric properties were investigated as a function of the x value and sintering temperatures. A single tilted orthorhombic perovskite structure in space group Pnma was refined in the studied composition range. For microware dielectric properties, the decreasing relative permittivity was strongly affected by the ionic polarizability of Nd^{3+} and Al^{3+} in SCNTAx ceramic systems. Also, the quality factor of SCNTAx solid solution had strongly depended on apparent densities and average grain sizes. As expected, the promising ceramic of SCNTAx ($x = 0.25$) sintered at 1520 °C for 4 h was found to possess good microwave dielectric properties: a relative permittivity (ε_r) of 55.6, a quality factor ($Q \times f$) of 25,600 GHz (at 4.249 GHz) and a temperature coefficient of resonant frequency (τ_f) of 6.7 ppm/°C. Especially, the τ_f values of SCNTAx ceramics were not strongly depended on tolerance factor (t) with increasing of the $NdAlO_3$ content, while these τ_f values were essentially correlated with the B-site bond valence and octahedral tilting. Wherein, either decreasing the B-site bond valence or increasing the octahedral tiltings (θ and φ) led to a decrease in τ_f value for the present ceramics.

1 Introduction

With the rapid development of mobile and satellite communication, microwave electronic devices are required to be developed and fabricated for miniaturization and integration. Particularly, as the typical representative of perovskite paraelectric titanates (ABO_3 structure), $CaTiO_3$ has been attracted much attention as microwave dielectric because of its high relative permittivity (~170) [1, 2]. However, its dielectric loss ($1/Q$) is rather high, compared with the complex perovskites. Thus, much work has been performed to control the microwave dielectric loss in $CaTiO_3$ through A-site substitution, such as $Ca_{1-x}Ln_{2x/3}TiO_3$ (Ln = La, Nd and Sm, $Q \times f \sim$ 8000–12,000 GHz) [3–5]. But their temperature coefficient of resonant frequency ($\tau_f \sim$ 190–440 ppm/°C) are too large to apply those microwave frequency devices, so that much attention has to paid to improve their temperature stability by mixing $CaTiO_3$-based materials with those materials (ABO_3) of negative τ_f value. Among these candidates, $CaTiO_3$–$NdGaO_3$ and $CaTiO_3$–$LaAlO_3$ ceramic systems are attracting great interests due to their better microwave dielectric properties ($\varepsilon_r \sim$ 35–45, $Q \times f \geq$ 33,000 GHz and $\tau_f \approx$ 0 ppm/°C) [6–8]. However, it is well known that a higher ε_r can facilitate circuit miniaturization because the wavelength inside the dielectric resonators (DRs) is inversely proportional to the square root of its ε_r. Although the good temperature stability and the lower dielectric loss can be obtained in those ceramics, the relative permittivity (ε_r) is not still high enough and can not meet the miniaturization for the high-

✉ Fei Liu
liufeiguet@163.com

[1] Department of Computer Science and Engineering, Guilin University of Aerospace Technology, Guilin 541004, People's Republic of China

[2] College of Material Science and Engineering, Guilin University of Electronic Technology, Guilin 541004, People's Republic of China

[3] College of Material Science and Engineering, Central South University, Changsha 410083, People's Republic of China

demand DRs. Therefore, it should be an important issue to further enhance the ε_r through the preparation of new dielectric ceramic materials.

$SrTiO_3$ is a well-known incipient ferroelectric with cubic perovskite structure at room temperature, and it possesses a higher relative permittivity ($\varepsilon_r \sim 270$), a modest quality factor ($Q \times f \sim 3{,}000$ GHz) and a larger temperature coefficient of resonant frequency ($\tau_f \sim 1650$ ppm/°C) [2, 9], compared with that of $CaTiO_3$. High relative permittivity makes it possible to noticeably miniaturize passive microwave components. Therefore, for practical application, some researchers have become increasingly interested in microwave dielectric properties of the $SrTiO_3$ series materials [10, 11]. In our previous work [12], the (Sr, Ca, Nd)TiO_3 ceramic systems were synthesized to investigate their structure and microwave dielectric properties, wherein the Sr^{2+} substitutions for $(Ca_{0.61}Nd_{0.26})^{2+}$ in $(1-x)SrTiO_3$–$xCa_{0.61}Nd_{0.26}TiO_3$ (SCNTx) ceramics could form solid solution. Especially, the $(Sr_{0.3}Ca_{0.427}Nd_{0.182})TiO_3$ (SCNT) specimen sintered at 1400 °C for 4 h was an orthorhombic distorted perovskite-type microwave dielectric material with a moderate $\varepsilon_r \sim 145$ and a very high $Q \times f \sim 7900$ GHz. In addition, a relatively lower positive $\tau_f \sim 415.6$ ppm/°C, compared with that of $SrTiO_3$ and/or $CaTiO_3$, can also be obtained for this sample. This means that the SCNTx ceramics can ensure the higher ε_r, at the same time achieve a temperature-stable material by forming solid solutions with the microwave ceramics of high negative τ_f values. On the other hand, $NdAlO_3$ belongs to a distorted perovskite structure at room temperature with low $\varepsilon_r \sim 22.3$, but high $Q \times f \sim 58{,}000$ and negative $\tau_f \sim -33$ ppm/°C [13]. In that way, the higher positive τ_f of SCNTx can be suppressed to low or near-zero τ_f value with the addition of $NdAlO_3$. Therefore, the aim of this work was to obtain a relative high ε_r (≥55), good $Q \times f$ (≥25,000 GHz) and near-zero τ_f by synthesizing $(1-x)(Sr_{0.3}Ca_{0.427}Nd_{0.182})$-$TiO_3$–$xNdAlO_3$ (referred to hereafter as SCNTAx hereafter, $0.1 \le x \le 0.4$) ceramic systems. Moreover, the phase composition, microstructure, and sintering behavior of the SCNTAx ceramics were also investigated in composition range with $x = 0.1$–0.4. Specially, regulatory mechanism of the τ_f values with the change of tolerance factor (t), B-site bond valence ($\overline{V}_B$) and octahedral tiltings (θ and φ) were discussed in details as well.

2 Experimental

Specimens with $x = 0.1$, 0.2, 0.25, 0.3 and 0.4 of $(1-x)(Sr_{0.3}Ca_{0.427}Nd_{0.182})TiO_3$–$xNdAlO_3$ (SCNTAx) ceramics were prepared by the conventional solid state reaction method using high-purity reagent-grade raw materials (more than 99.9 %) of $CaCO_3$, $SrCO_3$, Nd_2O_3, Al_2O_3 and TiO_2. These materials were mixed according to the desired compositions and ground in distilled water for 24 h with ZrO_2 balls. The mixtures were dried and calcined at 1150 °C ($x = 0.1$, 0.2, 0.25, 0.3) and 1250 °C ($x = 0.4$) for 2 h. The calcined powders were then sieved by using a 100 and 200 mesh screen. The sieved powders with 5 wt% PVA as a binder were pressed into pellets 11.5 mm in diameter and 5.5–6.0 mm in thickness under a pressure of 150 MPa. Additionally, these pellets were preheated at 650 °C for 2 h to expel the binder, then sintered at 1450–1620 °C for 4 h in air.

The crystalline structure of the prepared samples was analyzed by an X-ray diffractometer (XRD, D8-Advance, Bruker, Germany). After spraying the surfaces, the microstructures of these sintered specimens were examined by scanning electron microscopy (SEM, S-4800, Hitachi, Japan) coupled with energy dispersive spectroscopy (EDS). Additionally, the bulk density of the sintered ceramics was evaluated from the dimensions and weight. The relative permittivity (ε_r) was measured using the Hakki-Coleman dielectric resonator method with $TE_{01\delta}$ resonant modes (Agilent E5230C) [14], and the quality factor was characterized by $Q \times f$ (Q = 1/dielectric loss, f = resonant frequency) value at 3.8 = 6.1 GHz, which were measured through the parallel plate method, as modified and improved by Courtney [15]. In addition, the temperature coefficient of the resonant frequency (τ_f) was measured by using a temperature chamber. Accordingly, these τ_f values were calculated by the following equation (Eq. 1) [16]:

$$\tau_f = \frac{\Delta f_0}{f_0 \Delta T} = \frac{f_{75} - f_{25}}{f_{25} \times 50} \quad (1)$$

where f_{75} and f_{25} represent the resonant frequencies at 75 and 25 °C, respectively.

3 Results and discussions

The room-temperature X-ray diffraction (XRD) patterns recorded from the $(1-x)(Sr_{0.3}Ca_{0.427}Nd_{0.182})TiO_3$–$xNdAlO_3$ (SCNTAx, $0.1 \le x \le 0.4$) ceramics sintered at 1550 °C for 4 h are illustrated in Fig. 1a. As shown, all peaks can be indexed based on $CaTiO_3$ (PDF#42-0423) with an orthorhombic Pbnm structure and no second phase is detected for all the specimens, indicating the formation of SCNTAx solid solution, even in the sample with $x = 0.4$. In addition, as shown in the Fig. 1b, the main diffraction peak (121) of the orthorhombic phase slightly shifts to a higher angle with increasing $NdAlO_3$ content. This is due to the fact that the ionic radii of Nd^{3+} (1.27 Å, CN = 12) is slightly larger than that of $(Sr_{0.3}Ca_{0.427}Nd_{0.182})^{2+}$ (1.235 Å,

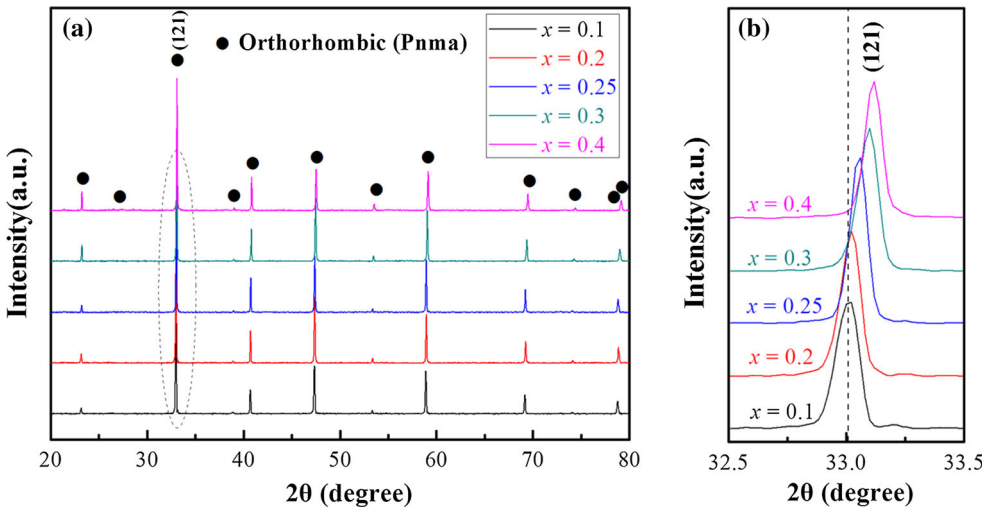

Fig. 1 **a** X-ray diffraction patterns of SCNTAx ($0.1 \leq x \leq 0.4$) ceramics sintered at 1550 °C for 4 h and **b** the magnified figure of (121) peak

CN = 12) at A-site, but the incorporation of the much smaller Al^{3+} (0.535 Å, CN = 6) in place of Ti^{4+} (0.605 Å, CN = 6) at B-site [17]. Thus, with an increase in the substitution of smaller Al^{3+}, all diffraction peaks gradually shift to the higher angles and the lattice parameters and unit cell volumes (Table 1) of the SCNTAx ceramics gradually decrease as well, which obeys the general known Vegard's law.

Figure 2 shows the back-scattered electron images (BEIs) of as-sintered surfaces of the SCNTAx ($0.1 \leq x \leq 0.4$) ceramics sintered at 1550 °C for 4 h. As shown in Fig. 2a–e, the color of all the grains is basically the same, which suggests that a single phase exists in the SCNTAx ceramics within the studied composition range, and this is a well agreement with the results of the XRD patterns (see Fig. 1a). In addition, a small amount of porosity and very small grains of 1–4 μm can be observed in Fig. 2a–c, and the small average grain size will result in a large amount of grain boundary, causing the low relative densities of the ceramics. Moreover, the average grain sizes increase with increasing $NdAlO_3$ content (see Fig. 2d, e), wherein a well-developed and uniform microstructure can be achieved by sintering the specimen with $x = 0.3$ at 1550 °C, it also means that 1550 °C may be the best densification sintering temperature for the SCNTAx ($x = 0.3$) sample.

Generally, the tolerance factor (t) is believed to be closely related with the temperature coefficient of resonant frequency (τ_f) in ABO_3 perovskite solid solutions, and the τ_f value increases linearly with an increasing of the tolerance factor if $t < 1$ [18, 19]. Wherein, the tolerance factor has been proposed and also defined as [20, 21]:

$$t = \frac{R_O + R_A}{\sqrt{2}(R_O + R_B)}, \tag{2}$$

where R_A is the radius of the A-site ion, R_B is the radius of B-site ion, and R_O is the radius of oxygen ion. However, our previous work (not be published) showed that the τ_f value in $(1-x)(Sr_{0.3}Ca_{0.427}Nd_{0.182})TiO_3$–$xSmAlO_3$ (SCNSTAx, $0.1 \leq x \leq 0.4$) ceramics sintered at 1480 °C for 4 h gradually decreased, while tolerance factor (t) of the SCNSTAx ceramics increased from 0.9307 to 0.9409 with increasing x value. This is due to the fact that the similarity of ionic radii between Sm^{3+} (1.24 Å, CN = 12) and $(Sr_{0.3}Ca_{0.427}Nd_{0.182})^{2+}$ (1.235 Å, CN = 12) at A-site is not enough to change the bending of B–O–B bond in adjacent BO_6 octahedra, as shown in Fig. 3a. When the size of A-site substitution is small enough, the tolerance

Table 1 B-site bond valence and lattice parameters of the SCNTAx ($0.1 \leq x \leq 0.4$) ceramics sintered at 1550 °C for 4 h

Composition	a (Å)	b (Å)	c (Å)	Cell volume (Å^3)	$\overline{R}_{B-O}$ (Å)	d_{B-O} (Å)	b (Å)	v_{B-O}	$\bar{V}_B$
$x = 0.1$	5.4274	7.6669	5.4234	225.67	1.7986	1.9167	0.37	0.7267	4.3602
$x = 0.2$	5.4245	7.6658	5.4202	225.39	1.7822	1.9164	0.37	0.6958	4.1748
$x = 0.25$	5.4236	7.6618	5.4123	224.91	1.7740	1.9155	0.37	0.6822	4.0932
$x = 0.3$	5.4175	7.6538	5.4082	224.25	1.7658	1.9135	0.37	0.6711	4.0266
$x = 0.4$	5.4092	7.6521	5.4120	224.01	1.7494	1.9130	0.37	0.6426	3.8556

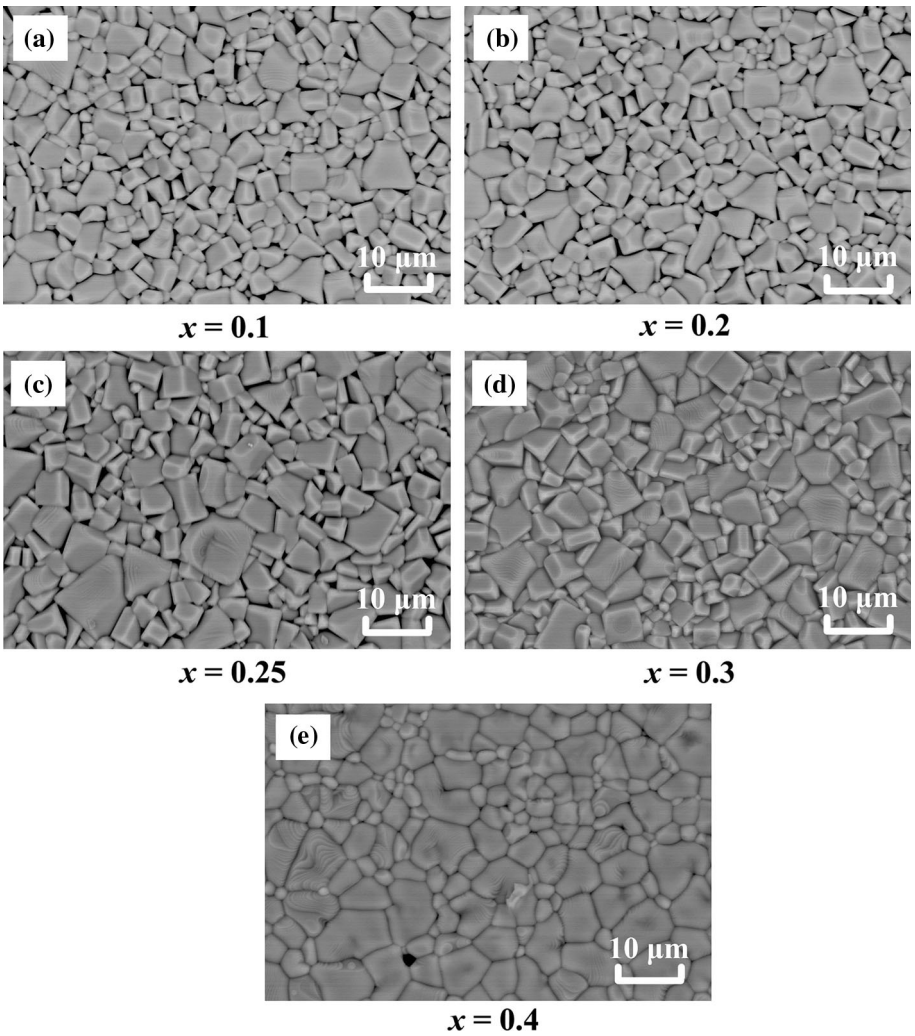

Fig. 2 Back-scattered electron images of as-sintered surfaces of the SCNTAx ($0.1 \leq x \leq 0.4$) ceramics sintered at 1550 °C for 4 h

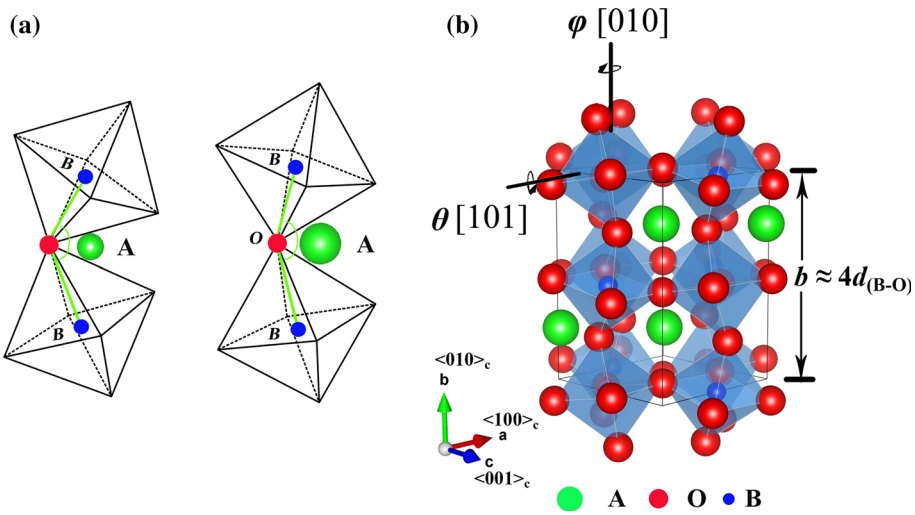

Fig. 3 **a** The relationship between large and/or small A-site ions and the bending of B–O–B bond in adjacent oxygen octahedra, **b** the distorted orthorhombic perovskite with a space group of Pnma derived through the octahedral tilting θ and φ

factor (t) can effectively reflect the structural stability in ABO_3 structure. Moreover, for SCNSTAx ceramic systems, the increasing t is attributed to the incorporation of smaller Al^{3+} (0.535 Å, CN = 6) in place of Ti^{4+} (0.605 Å, CN = 6) at B-site, but the substitution of Al^{3+} for B-site just results in an increase in the intensity of oxygen and

B-site ions at single BO_6 octahedra, which hardly impacts on the thermal stability of ceramic systems. An increase in tolerance factor (t) merely indicates that the volume of the BO_6 octahedron is better matched to the size of the AO_{12} polyhedron. In the present work, for the SCNTAx ceramics, the Eq. (2) becomes:

$$t = \frac{R_{O^{2-}} + 0.427(1-x)R_{Ca^{2+}} + 0.182(1-x)R_{Nd^{3+}} + 0.3(1-x)R_{Sr^{2+}} + xR_{Nd^{3+}}}{\sqrt{2}[R_{O^{2-}} + (1-x)R_{Ti^{4+}} + xR_{Al^{3+}}]}. \quad (3)$$

By calculating, the tolerance factor (t) gradually increases from 0.9317 at $x = 0.1$ to 0.9452 at $x = 0.4$, while the τ_f value also gradually declines according to the analysis below. These results are similar with that of SCNSTAx ceramics, and it also illustrates that the τ_f values are not strongly depended on tolerance factor (t) with increasing x value in SCNTAx ceramic systems. Thus, we consider that, without the phase transitions [22, 23], the τ_f value is closely related with the the size of A-site ions substitution and the bending of B–O–B bonds. It can be concluded that the increasement of the bending in B–O–B bonds means the higher stability and lower symmetry in ABO_3 perovskite structure. Also, it also indicates that the rattling effect in single BO_6 octahedra decreases, giving rise to a decrease in τ_f value.

On the other hand, the temperature coefficient of the resonant frequency (τ_f) strongly depends on B-site bond valence or octahedral tilting for ABO_3 perovskite structure [24–27]. The bond valences of B-site ($\overline{V}_B$) for the SCNTAx ceramics are calculated using the following equations [24, 28]:

$$\overline{V}_i = \sum v_{ij} \quad (4)$$

$$v_{ij} = \exp\left[\frac{\overline{R}_{ij} - d_{ij}}{b}\right], \quad (5)$$

where $\overline{R}_{ij}$ is the average bond valence parameter, d_{ij} is the length of a bond between atom i and j, and b is a universal constant (0.37 Å). In this work, the SCNTAx is an distorted orthorhombic perovskite with a space group of Pnma on a $\sqrt{2} \times \sqrt{2} \times 2$ cell in the investigational range with $x = 0.1$–0.4, and its d_{B-O} is approximately equal to $\frac{1}{4}b$ (lattice parameter) in an unit cell volume [29], as shown in Fig. 3b. Additionally, replacing Ti^{4+} with Al^{3+} in the SCNTAx ceramics will lead to a variation in the atomic interactions, which results in a change in bond valence of this material. Table 1 summarizes the B-site bond valences calculated using Eqs. (4), (5) and the relevant lattice parameters for the present SCNTAx ceramics. Meanwhile, Fig. 4 displays the τ_f value of the SCNTAx ($0.1 \le x \le 0.4$) ceramics sintered at 1550 °C for 4 h as a function of B-site bond valences. As can be seen from Fig. 4, the τ_f value gradually shifts to near zero or negative direction with a decrease in $\overline{V}_B$ as x value increases from 0.1 to 0.4. According to the bond valence theory [28], the shorter the bond length is, the stronger the bond energy become, which also explains that the rattling effect of B-site cation is decreased, thus causing τ_f value to decrease. Moreover, the tilting of octahedra is another important parameters related to the τ_f value of ABO_3 perovskites that significantly affect the stability of crystal structure. The orthorhombic Pnma in these SCNTAx systems gives a tilt system of $a^-b^+a^-$ by using Glazer's notation [21], meaning that there are two approximately equal anti-phase tilts about the a axis and an in-phase tilt about the b axis. It can also be conceived as the result of tiltings (θ and φ) about the [101] and [010] orientations of the regular octahedra (see Fig. 3b). Additionally, the unit cell parameters are related to the octahedral tiltings and bond valence parameters through the following relationships [30]:

$$\cos\theta = 1 - \frac{\left|2\sqrt{2} \times \bar{R}_{B-O} - a\right|}{2\sqrt{2} \times \bar{R}_{B-O}} \quad (6)$$

$$\cos\varphi = 1 - \frac{\left|4 \times \bar{R}_{B-O} - b\right|}{4 \times \bar{R}_{B-O}}, \quad (7)$$

where $\overline{R}_{ij}$ is the same as that of Eq. (2). Figure 4 also shows that the $NdAlO_3$-addition increases octahedral tiltings (θ and φ) from 21.09° to 24.90°, and from 20.77° to 24.97°, affecting a reduction in τ_f value of the SCNTAx ceramics from 132.8 to −19.5 ppm/°C. These results can be attributed to the fact that the increasing octahedral tilting results in a corresponding increase in the restoring force for recovering the tilting, and this stronger restoring force can inhibit the increase of heat effect and suppress the ionic rattling of A- and B-sites in a certain degree [27, 31], then the τ_f value accordingly decreases. Therefore, the temperature coefficient of the resonant frequency (τ_f) can be effectively evaluated by the B-site bond valences and octahedral tilting for these SCNTAx ($0.1 \le x \le 0.4$) perovskite ceramics.

Figure 5 illustrates the relative permittivity (ε_r) of SCNTAx ($0.1 \le x \le 0.4$) ceramics sintered at various

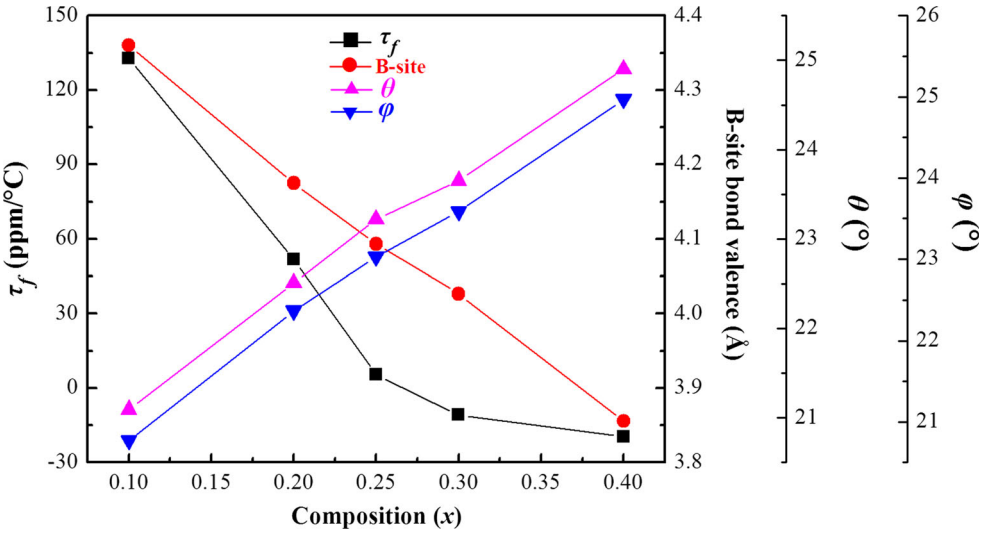

Fig. 4 τ_f value of the SCNTAx ($0.1 \leq x \leq 0.4$) ceramics sintered at 1550 °C for 4 h as a function of B-site bond valence and octahedral tiltings (θ and φ)

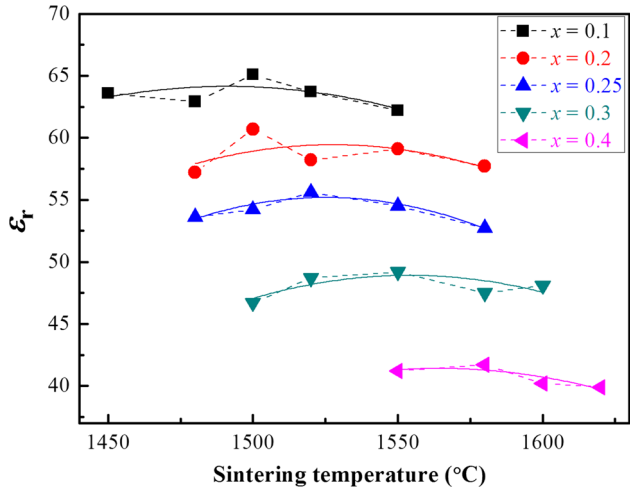

Fig. 5 ε_r of the SCNTAx ($0.1 \leq x \leq 0.4$) ceramics as functions of various sintering temperatures for 4 h

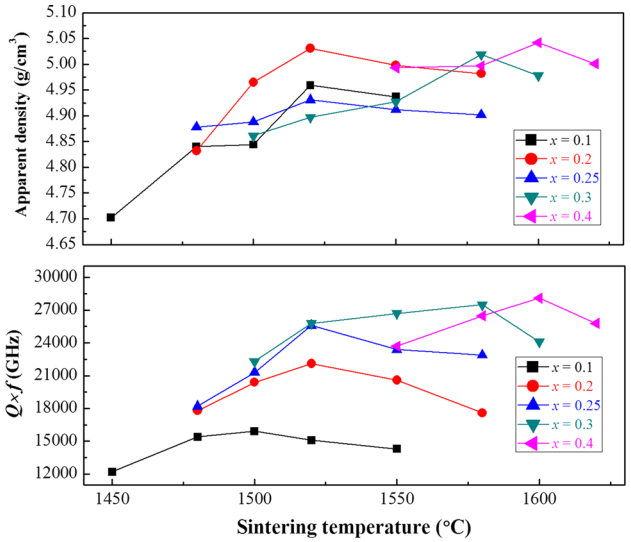

Fig. 6 **a** Apparent density and **b** room-temperature $Q \times f$ value of the SCNTAx ($0.1 \leq x \leq 0.4$) ceramics as a function of sintering temperature for 4 h

sintering temperatures (1450–1620 °C) for 4 h with different x value. It can be found that the ε_r decreases steadily from 62.2 to 41.2 with the increase of $NdAlO_3$ content when sintering temperature is 1550 °C. We approve that the relative permittivity is strongly dependent on the ionic polarizability for ABO_3 perovskite solid solutions materials [25, 32]. For the present SCNTAx ($0.1 \leq x \leq 0.4$) solid solutions, although $(Sr_{0.3}Ca_{0.427}Nd_{0.182})^{2+}$ has a similar ionic polarizability (3.53 Å^3) than that of Nd^{3+} (5.01 Å^3), the ionic polarizability of Al^{3+} (0.79 Å^3), however, is much lower than that of Ti^{4+} (2.93 Å^3). Therefore, the ε_r decreases gradually with an increasing of x value on account of the fact that the integral dielectric polarizability of $NdAlO_3$ (11.83 Å^3) is smaller than that of SCNT (12.49 Å^3) [33]. In addition, as shown, the ε_r are not affected greatly by sintering temperatures in the same x value, and a maximum ε_r value of ~55.6 is obtained for the specimen using SCNTAx ($x = 0.25$) sintered at 1520 °C for 4 h. Moreover, thses ranges in sintering temperature of the SCNTAx ceramics increase from 1450–1550 °C at $x = 0.1$ to 1550–1620 °C at $x = 0.4$ because $NdAlO_3$ requires a higher sintering temperature of ~1650 °C [13].

Figure 6a shows the apparent density of SCNTAx ($0.1 \leq x \leq 0.4$) ceramics sintered at different sintering temperature for 4 h. It can be observed that, for the same x value, the specimens' apparent densities initially increase with increasing sintering temperature and reach a maximum, then slightly decrease at a further increasing sintering temperature. On the other hand, the room-temperature $Q \times f$ values of the

SCNTAx ($0.1 \leq x \leq 0.4$) ceramics sintered at 1450–1620 °C for 4 h are demonstrated in Fig. 6b. As reported, the $Q \times f$ value strongly depends on the extrinsic factors, such as second phase, density, and grain size [34, 35]. In these SCNTAx ceramic systems, the effects of the secondary phase can be neglected, because the secondary phase in SCNTAx solid solution is not detected through the investigated composition range with $x = 0.1$–0.4, as confirmed in Fig. 1. As expected, an ordinary behavior is found that the $Q \times f$ value is inside the range exhibited by the end members SCNT with a $Q \times f$ value of 7900 GHz and $NdAlO_3$ with a $Q \times f$ value of 58,000 GHz. In addition, the variation in $Q \times f$ value of SCNTAx (except $x = 0.1$) ceramics is basically consistent to that of the apparent density with the increasing sintering temperature, and the higher density means the lower porosity, producing a decrease in dielectric loss of the ceramic systems [36]. As a result, the $Q \times f$ value is also mainly controlled by the microstructure in the present ceramics. Although the $Q \times f$ value increases gradually with an increase in x value due to the higher $Q \times f$ value of $NdAlO_3$, a slow increase in $Q \times f$ values for the samples with $x = 0.3$ and 0.4 is shown in Fig. 6b. It can be explained by that large grains in dielectric ceramics usually contain more defects, such as dislocations, planar defects, and even the dislocation networks, which can lead to a decrease in the $Q \times f$ value to some extent [31, 37]. Therefore, the increasing extent of $Q \times f$ value in SCNTAx ($0.1 \leq x \leq 0.4$) ceramics is decreased due to the increasing average grain sizes, as shown in Fig. 2a–e.

4 Conclusions

The microstructure, phase composition and microwave dielectric properties of $(1 - x)(Sr_{0.3}Ca_{0.427}Nd_{0.182})TiO_3$–$xNdAlO_3$ (SCNTAx, $0.1 \leq x \leq 0.4$) ceramics were investigated in this work. The XRD results showed that the single orthorhombic perovskite solid solution could be formed in the composition range of $x = 0.1$–0.4. Also, a temperature-stable mechanism of these SCNTAx ceramics at microwave frequency were also explained through the tolerance factor (t), B-site bond valence and octahedral tiltings. Wherein, the τ_f values of SCNTAx ceramics were not strongly depended on tolerance factor ($t < 1$) with increasing of the $NdAlO_3$ content, but on the bending of B–O–B bond at adjacent BO_6 octahedron for ABO_3 perovskite structure. On the other hand, these τ_f values were essentially correlated with the B-site bond valence and octahedral tilting, and either decreasing the B-site bond valence or increasing the octahedral tiltings (θ and φ) led to a decrease in τ_f value for these ceramic systems. Moreover, ε_r decreased with increasing x value due to the smaller dielectric polarizability of $NdAlO_3$ than that of SCNT, and the $Q \times f$ value in SCNTAx solid solution had strongly depended on the apparent density and average grain sizes. As a result, excellent microwave dielectric properties of $\varepsilon_r \sim 55.6$, $Q \times f \sim 25{,}600$ GHz (at 4.249 GHz) and $\tau_f \sim 6.7$ ppm/°C were obtained for SCNTAx ($x = 0.25$) ceramic sintered at 1520 °C for 4 h, which is a promising candidate for miniaturization components in developing wireless communication systems.

Acknowledgments Financial supports of the National Natural Science Foundation of China (Grant No. 11464006), the Natural Science Foundation of Guangxi (Grant No. 2014GXNSFBA118254).

References

1. F. Liang, M. Ni, W.Z. Lu et al., Crystal structure and microwave dielectric properties of $CaTiO_3$–$La[Ga_{(1-\delta)}Al_\delta]O_3$ ceramics system. Mater. Res. Bull. **57**, 140–145 (2014)
2. P.L. Wise, I.M. Reaney, W.E. Lee et al., Structure microwave property relations in $(Sr_xCa_{1-x})_{n+1}Ti_nO_{3n+1}$. J. Eur. Ceram. Soc. **21**, 1723–1726 (2001)
3. I.S. Kim, W.H. Jung, Y. Inaguma et al., Dielectric properties of A site deficient perovskite type lanthanum-calcium-titanium oxide solid solution system $(1 - x)La_{2/3}TiO3$–$xCaTiO_3$ ($0.1 \leq x \leq 0.96$). Mater. Res. Bull. **30**, 307–316 (1995)
4. M.S. Fu, X.Q. Liu, X.M. Chen, Structure and microwave dielectric characteristics of $Ca_{1-x}Nd_{2x/3}TiO_3$ ceramics. J. Eur. Ceram. Soc. **28**, 585–590 (2008)
5. W.S. Kim, E.S. Kim, K.H. Yoon, Effects of Sm^{3+} substitution on dielectric properties of $Ca_{1-x}Sm_{2x/3}TiO_3$ ceramics at microwave frequencies. J. Am. Ceram. Soc. **82**, 2111–2115 (1999)
6. M.H. Kim, S. Nahm, C.H. Choi et al., Dielectric properties of $(1 - x)NdGaO_3$–$xCaTiO_3$ solid solution at microwave frequencies. Jpn. J. Appl. Phys. **41**, 717–721 (2002)
7. H.X. Yuan, X.M. Chen, M.M. Mao, Structure and microwave dielectric characteristics of $Ca_{1+x}Nd_{1-x}Al_{1-x}Ti_xO_4$ ceramics. J. Am. Ceram. Soc. **92**(10), 2286–2290 (2009)
8. D.D. Khalyavin, A.N. Salak, A.M.R. Senos et al., Ferreira Structure sequence in the $CaTiO_3$–$LaAlO_3$ microwave ceramics-revised. J. Am. Ceram. Soc. **89**(5), 1721–1723 (2006)
9. R.C. Kell, A.C. Greenham, G.C.E. Olds, High-permittivity temperature-stable ceramic dielectrics with low microwave loss. J. Am. Ceram. Soc. **56**(7), 352–354 (1974)
10. C.J. Howard, G.R. Lumpkin, R.I. Smith et al., Crystal structures and phase transition in the system $SrTiO_3$–$La_{2/3}TiO_3$. J. Solid. State. Chem. **177**, 2726–2732 (2004)
11. C.L. Huang, K.H. Chiang, Dielectric properties of B_2O_3 doped (1–x)$LaAlO_3$–x$SrTiO_3$ ceramic system at microwave frequency range. Mater. Res. Bull. **37**, 1941–1948 (2002)
12. F. Liu, C.L. Yuan, X.Y. Liu et al., Microstructures and dielectric properties of $(1 - x)SrTiO_3$–$xCa_{0.61}Nd_{0.26}TiO_3$ ceramic system at microwave frequencies. J. Mater. Sci.: Mater. Electron. **26**(1), 128–133 (2015)
13. S.Y. Cho, I.T. Kim, K.S. Hong, Microwave dielectric properties and applications of rare earth aluminates. J. Mater. Res. **14**, 114–119 (1999)
14. B. Hakki, P. Coleman, A dielectric resonator method of measuring inductive capacities in the millimeter range. IEEE Trans. Microwave Theory Tech. MTT **8**, 402–410 (1960)
15. W. Courtney, Analysis and evaluation of a method of measuring complex permittivity and permeability of microwave materials. IEEE Trans. Microwave Theory Tech. MTT **18**, 476–485 (1970)

16. T. Nishikawa, K. Wakino, H. Tamura et al., Precise measurement method for temperature coefficient of microwave dielectric resonator material. IEEE MTT-S Int. Microwave Symp. Dig. **3**, 277–280 (1987)
17. R.D. Shannon, Revised effective ionic radii and systematic studies of interatomic distances in halides and chalcogenides. Acta. Cryst. A **32**, 751–767 (1976)
18. M. Reaney, E.L. Colla, N. Setter, Dielectric and structural characteristics of Ba and Sr based complex perovskites as a function of tolerance factor. Jpn. J. Appl. Phys. **33**, 3984–3990 (1994)
19. I.M. Reaney, R. Ubic, Dielectric and structural characteristics of perovskites and related materials as a function of tolerance factor. Ferroelectrics **228**, 23–38 (1999)
20. A.M. Glazer, The classification of tilted octahedral perovskites. Acta. Cryst. **B28**, 3384–3392 (1972)
21. A.M. Glazer, Simple ways of determining perovskite structures. Acta. Cryst. **A31**, 756–762 (1975)
22. L.A. Khalam, M.T. Sebastian, Microwave dielectric properties of $Sr(B'_{1/2}Nb_{1/2})O_3$ [B' = La, Pr, Nd, Sm, Eu, Gd, Tb, Dy, Ho, Y, Er, Yb and In] ceramics. Int. J. Appl. Ceram. Tech. **3**, 364–374 (2006)
23. L.A. Khalam, M.T. Sebastian, Low loss dielectrics in the $Ca(B'_{1/2}B''_{1/2})O_3$ [B' = lanthanides, *y*] system. J. Am. Ceram. Soc. **90**, 1467–1474 (2007)
24. W.R. Yang, C.C. Pan, C.L. Huang, Influence of Mg substitutions for Zn on the phase relation and microwave dielectric properties of $(Zn_{1-x}Mg_x)_3Nb_2O_8$ (x = 0.02–1.0) system. J. Alloys. Comp. **581**, 257–262 (2013)
25. E.S. Kim, B.S. Chun, D.W. Yoo et al., Microwave dielectric properties of $(1-x)(Ca_{0.7}Nd_{0.2})TiO_3$–$x(Li_{0.5}Nd_{0.5})TiO_3$ ceramics. Mater. Sci. Eng. B **99**, 247–251 (2003)
26. J. Qu, C. Yuan, F. Liu et al., Microstructures and microwave dielectric properties of $(1-x)Sr_{0.2}Na_{0.4}Sm_{0.4}TiO_3$–$x$LnAlO$_3$ (Ln = Nd, Pr and Sm) ceramic systems. J. Mater. Sci.: Mater. Electron. **26**(7), 4862–4869 (2015)
27. E.S. Kim, E.S. Chun, D.H. Kang, Effects of structural characteristics on microwave dielectric properties of $(1-x)Ca_{0.85}Nd_{0.1}TiO_3$–$x$LnAlO$_3$ (Ln = Sm, Er and Dy) ceramics. J. Eur. Ceram. Soc. **27**, 3005–3010 (2007)
28. N.E. Brese, M. O'Keeffe, Bond-valence parameters for solids. Acta. Cryst. **B47**, 192–197 (1991)
29. M. Yashima, R. Ali, Structural phase transition and octahedral tilting in the calcium titanate perovskite $CaTiO_3$. Solid State Ionics **180**, 120–126 (2009)
30. Y.S. Zhao, Crystal chemistry and phase transitions of perovskite in *P*–*T*–*X* space: data for $(K_xNa_{1-x})MgF_3$ perovskite. J. Solid State Chem. **141**, 121–132 (1998)
31. J.M. Li, Y.X. Han, T. Qiu et al., Effect of bond valence on microwave dielectric properties of $(1-x)CaTiO_3$–$x(Li_{0.5}La_{0.5})TiO_3$ ceramics. Mater. Res. Bull. **47**, 2375 (2012)
32. J.J. Qu, F. Liu, X. Wei et al., New dielectric material systems of $Sr_xNd_{2(1-x)/3}TiO_3$ perovskites-like at microwave frequencies. Mater. Chem. Phys. **173**, 309–316 (2016)
33. R.D. Shannon, Dielectric polarizabilities of ions in oxides and fluorides. J. Appl. Phys. **73**(1), 348–366 (1993)
34. F. Zhao, Z.X. Yue, Y.Z. Lin et al., Phase relation and microwave dielectric properties of xCaTiO$_3$–$(1-x)$TiO$_2$–3ZnTiO$_3$ multiphase ceramics. Ceram. Int. **33**, 895–900 (2007)
35. C.H. Hsun, C.H. Chang, A temperature-stable and high-Q microwave dielectric ceramic of the $MgTiO_3$–$(Ca_{0.8}Sr_{0.2})(Zr_{0.1}Ti_{0.9})O_3$ system. Ceram. Int. **41**, 6965–6969 (2015)
36. C.H. Hsun, S.H. Tsai, Dielectric characteristics of Sr substitution on $Ca_{0.4}Sm_{0.4}TiO_3$ ceramics at microwave frequency. Ceram. Int. **40**, 10111–10114 (2014)
37. J.M. Li, T. Qiu, Microwave dielectric properties of $(1-x)Ca_{0.6}La_{0.267}TiO_3$–$xCa(Sm_{0.5}Nb_{0.5})O_3$ ceramics. Ceram. Int. **38**, 4331–4335 (2012)